Hetero-bimetallic Lanthanide-Coinage Metal Compounds Featuring Possible Metal-Metal Interactions in the Excited State

Milena Dahlen[+],[a] Niklas Reinfandt[+],[a] Chengyu Jin,[b] Michael T. Gamer,[a] Karin Fink,[b] and Peter W. Roesky*[a]

In memory of Professor Markus Gerhards

Abstract: Heterometallic complexes, combining metals of the outer rims of the d-block, for example lanthanides(III) (Ln) and coinage metals(I) (M) are scarcely reported, synthetically challenging and highly interesting in terms of their interactions. In this context, we synthesized hetero-bimetallic Ln–M compounds ligated by the phosphine functionalized amidinate system (*N*,*N*′-bis[(2-diphenylphosphino)phenyl] formamidinate, "dpfam"). The resulting compounds [dpfam$_3$LnM][OTf] (Ln = La, Nd and M = Ag, Au) feature a close proximity of the two metal centres and were investigated experimentally by photoluminescence spectroscopy and quantum chemical calculations. The latter showed rare La–Au interactions for the first excited state.

Introduction

Heterometallic compounds exhibiting narrow intermetallic distances have been of rising interest over recent decades. Known for their potential synergistic effects arising from cooperative metal-metal interaction, they pose a promising class of compounds in various fields of application such as catalysis, luminescence, small molecule activation and others.[1] Interesting compounds in this context are for example early-late transition metal complexes (ELTM). Combining a usually highly charged hard (referring to Pearson's HSAB principle)[2] early transition metal cation with a rather soft late metal cation in a low oxidation state, they provide both – opportunities and challenges. For example, in terms of catalysis a combination of different metal centres could alter the reactivity towards substrates and might enable new reaction pathways.[1a,b]

However, combination of such differently charged metal centres provides challenges: a suitable ligand design to overcome the repulsion of two charged metal centres and the intrinsic difficulty of possible intermetallic redox reactions.

Especially in terms of luminescence, such heterometallic compounds which combine a metal with an empty d-shell but open f-shell (e.g., lanthanides; Ln) and a metal with a fully occupied but chemical still accessible d-shell (e.g., coinage metals) are a promising research field. Lanthanides have been known for their luminescence properties ever since.[3] They represent an essential component in the design of luminescent materials, for example organic LEDs and doped materials.[4] With the origin of their luminescence being well established, they would be an obvious choice for such a heterometallic model complex in terms of fundamental luminescence research.[3b,5] Coinage metals on the other hand have been known for around three decades in context of cooperativity as they readily undergo short metal–metal distances, commonly known as "metallophilicity".[6] Additionally, they often feature distinct photoluminescent properties resulting from an alteration of LMCT→LMMCT and heavy metal effects (LM(M)CT = ligand to metal (metal) charge transfer).[7]

However, although various examples of heterometallic lanthanide compounds[8] with transition metals and short intermetallic distances or metal-metal interactions (e.g., Lu–Ni,[9] Ln–Rh (Ln = La, Ce, Nd),[10] Nd–Pd,[11] Ln–M (Ln = Y, Lu, M = Pd, Pt))[12] and even unsupported Ln–M bonds are known,[13] examples with the coinage metals (M = Cu, Ag, Au), especially with Ln–M distances $\leq$4 Å, are still very rare and could not show any direct Ln–M interactions so far.[14] Therefore, we felt challenged to assemble in a molecular approach

[a] M. Dahlen,[+] N. Reinfandt,[+] Dr. M. T. Gamer, Prof. Dr. P. W. Roesky
Institute for Inorganic Chemistry
Karlsruhe Institute of Technology
Engesserstr. 15, Geb. 30.45, 76131 Karlsruhe (Germany)
E-mail: roesky@kit.edu

[b] C. Jin, Prof. Dr. K. Fink
Institute of Nanotechnology
Karlsruhe Institute of Technology
Hermann-von-Helmholtz-Platz 1
76344 Eggenstein-Leopoldshafen (Germany)

[+] These authors contributed equally to this work.

Supporting information for this article is available on the WWW under https://doi.org/10.1002/chem.202102430

This manuscript is part of a Special Issue "Cooperative effects in heterometallic complexes".

coinage metals and lanthanides within close proximity and to study their interaction in ground and excited state.

As ligand we chose an established PNNP ligand system (*N*,*N*′-bis[(2-diphenylphosphino)phenyl]formamidinate, "dpfam")[15] featuring different coordination compartments especially designed for the selective coordination of hard and soft metal ions (Figure 1).

We have used the dpfam ligand previously for the synthesis of bimetallic coinage metal complexes (Figure 2).[15f,g] Following the concept shown in Figure 1, Au^{I} ions exclusively bind to P atoms while Cu^{I} and Ag^{I} are N- and P-coordinated.[15g]

Results and Discussion

For the synthesis of the target complexes, we followed a two-step protocol. As a first step, the potassium salt of the ligand (Kdpfam) which exhibits a polymeric structure in the solid state was coordinated to the lanthanide metal via the amidinate function (Scheme 1). In a second step, the resulting lanthanide complexes were treated with coinage metal precursors to generate the desired bimetallic compounds.

For initial experiments Tb was chosen as suitable lanthanide due to its well investigated luminescence properties.[16] Salt metathesis of $TbCl_3$ with 3 equivalents of Kdpfam resulted in [$dpfam_3Tb$] (**1**), which was isolated as almost colourless crystals in yields of 61 % (Scheme 2). Single crystal X-ray analysis revealed the terbium cation being coordinated by both nitrogen atoms and one phosphorus atom of each of the three ligands, resulting in a ninefold coordination (Figure 3) that could best be described as a muffin polyhedron (SHAPE 2.1).[17] Within the complex, there are four planes of three donor atoms each ($P1_3$, $N1_3$, $N2_3$, $P2_3$), each of which lies parallel to the other (Figure 5). The two N–Tb bonds are slightly different and slightly (~0.1 Å) longer than comparable values in the literature.[18]

Owing to the similar N1–C1 and N2–C1 bond lengths, a delocalization of the negative charge between the nitrogen atoms can be assumed. The N–C–N angle was determined to be 115.7(7)°. The Tb–P distances are in comparison to other Ln–P bonds relatively long (3.213(2) Å),[19] presumably due to the relatively stiff N–aryl–P fragment within the ligand. In the representation of the solid-state structure of **1** in Figure 3, the free coordination pocket, stretched by the three free phosphorus atoms, is highlighted in blue. Despite various attempts, this position could not be occupied by another metal. While for silver and gold no products were obtained, experiments with copper resulted in the isolation of the correspond-

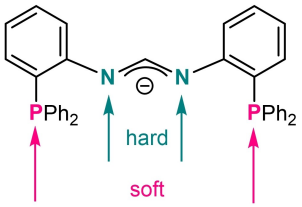

Figure 1. The dpfam ligand featuring different coordination compartments especially designed for the selective coordination of hard and soft metal ions.

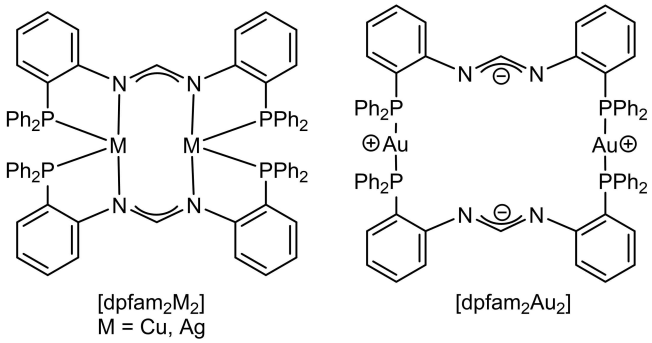

Figure 2. Previously obtained coinage metal compounds with dpfam.[15g]

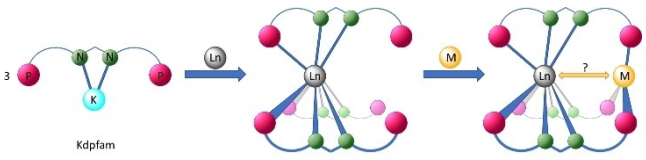

Scheme 1. Schematic drawing of the synthetic approach to binuclear lanthanide/coinage metal complexes.

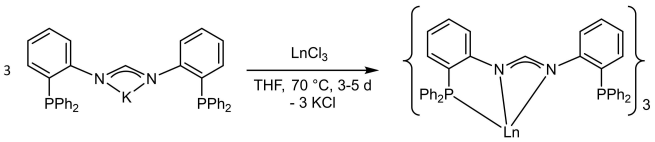

Ln = Tb (**1**), La (**2**), Nd (**3**)

Scheme 2. Synthesis of [$dpfam_3Ln$] with Ln = Tb (**1**), La (**2**) and Nd (**3**).

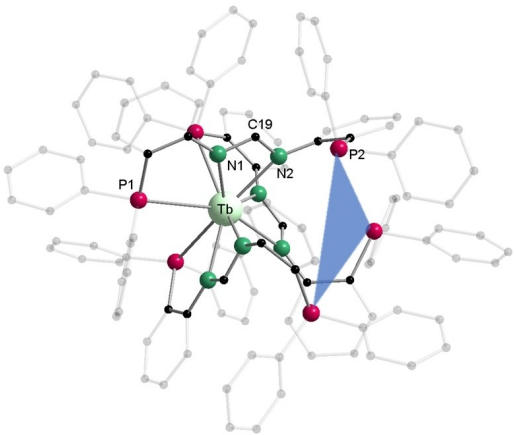

Figure 3. Molecular structure of **1** in the solid state. Protons and non-coordinating solvents are omitted for clarity. Selected bond lengths [Å] and angles [°]: Tb–P1 3.213(2), Tb–N1 2.450(6), Tb–N2 2.512(7), N1–C19 1.345(10), N2–C19 1.295(10), N1–C19–N2 115.7(7).

ing Cu_2 compound [dpfam$_2$Cu$_2$] (Figure 2).[15g] This lead to the conclusion that the comparatively hard Cu^+ ion seems to cast out the lanthanide from the amidinate pocket.

Obviously, the remaining coordination pocket in **1** is either too small or too stiff to host a silver(I) or gold(I) cation. Therefore, we moved to the larger lanthanides La and Nd. While La is a closed shell system, which allows for NMR spectroscopic investigations, Nd is known for its distinct emission in the IR range. The desired homoleptic dpfam complexes [dpfam$_3$La] (**2**) and [dpfam$_3$Nd] (**3**) were synthesized analogously to **1** by a salt metathesis (Scheme 2). Compounds **2** and **3**, which are isostructural (Figure 4), were isolated in 63% and 56% crystalline yield.

As observed for **1**, the lanthanide atoms in **2** and **3** are ninefold coordinated by six N and three P atoms forming a spherical tricapped trigonal prism polyhedron (SHAPE 2.1).[17] Due to the larger ion radius and the different coordination polyhedron the solid state structure shows the position of the lanthanide ion to be slightly more central within the P_3^N_6^P_3 cage, compared to **1**. Hence, the in **1** observed P_3 coordination pocket is not visible for **2** and **3**, but again three out of six phosphorus atoms are non-coordinating. The Nd–N bonds average to 2.55 Å, the La–N bonds correspondingly to 2.61 Å, and are both slightly longer than already reported bond lengths.[20]

Due to low solubility and some dynamics, the NMR spectra show a better resolution at elevated temperature. High temperature (323 K) $^{31}P\{^1H\}$ NMR spectroscopy of **2** in THF-d_8 resulted in one broad main resonance at $\delta = 14.0$ ppm. For the synthesis of the desired bimetallic complexes, Ag^+ and Au^+ precursors were successfully reacted with the lanthanide precursors **2** and **3**, while reaction with the harder ion Cu^+ failed. Reaction of **2** and **3** with AgOTf in THF resulted in the hetero-bimetallic compounds [dpfam$_3$LaAg][OTf] (**4**) and [dpfam$_3$NdAg][OTf] (**5**, Scheme 3). Due to the coordination of the Ag^+ ion, the coordination sphere of the lanthanide atoms is rearranged and a coordination pocket for the Ag^+ ion is formed. In both complexes, the lanthanide cations are in the centre of a muffin polyhedron as observed in the Tb compound **1**. The lanthanide atoms in **4** and **5** are ninefold coordinated by a P_3 unit and the six nitrogen atoms of the amidinates. The P_3 and N_3 planes are nearly parallel to each other and only slightly tilted (maximum of 2.54° for **4**) (Figures 5 and 6). Compared to their respective reactants, the Ln–N bond lengths hardly change (∅(La–N) = 2.61 Å, (∅(Nd–N) = 2.54 Å).

The silver cation is coordinated in an almost trigonal planar manner (P–Ag–P: **4**: 117.09(3), 116.57(3), 117.95(3) **5**: 116.60(2)°) – a structural motif that has been observed rather rarely for silver.[21] The distance of the silver atom from the P_3 plane accounts to 0.42 Å (**4**) and 0.46 Å (**5**).

The corresponding P–Ag bonds have approximately the same length in both complexes (**4**: (∅(Ag–P) = 2.487 Å, **5**: P–Ag 2.4926(14) Å) and fit into the literature values of the corresponding coordination motif (Figure 6).[21]

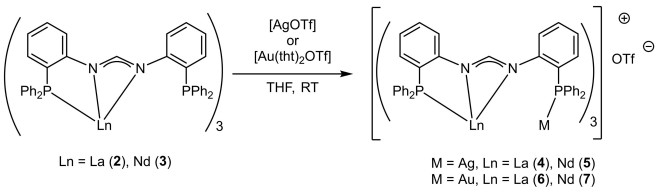

Scheme 3. Synthesis of the heterometallic compounds [dpfam$_3$LnM][OTf] **4**–**7**.

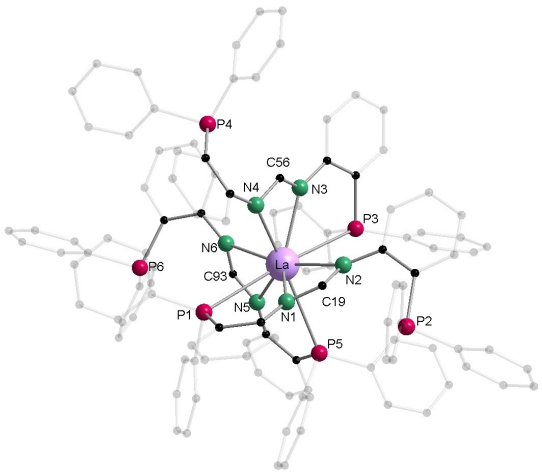

Figure 4. Molecular structure of **2** in the solid state. Compound **3** is isostructural (Figure S25). Protons and non-coordinating solvents are omitted for clarity. Selected bond lengths [Å] and angles [°] for **2** and **3**: **2**: La–P1 3.2473(10), La–P3 3.3267(10), La–P5 3.3192(10), La–N1 2.567(3), La—N2 2.630(3), La–N3 2.608(3), La–N4 2.610(3), La–N5 2.570(3), La–N6 2.650(3), N1–C19 1.333(4), C19–N2 1.324(4), N3–C56 1.323(4), C56–N4 1.309(4), N5–C93 1.329(4), N6–C93 1.314(4), N2–C19–N1 117.8(3), N3–C56–N4 118.9(3), N5–C93–N6 118.4(3). **3**: Nd–P1 3.290(2), Nd–P3 3.297(2), Nd–P5 3.188(2), Nd–N1 2.499(5), Nd–N2 2.604(6), Nd–N3 2.548(5), Nd–N4 2.563(6), Nd–N5 2.501(5), Nd–N6 2.575(5), N1–C19 1.338(9), C19–N2 1.314(8), N3–C56 1.327(8), C56–N4 1.318(9), N5–C93 1.335(8), N6–C93 1.314(8), N2–C19–N1 117.9(6), N3–C56–N4 119.1(6), N5–C93–N6 117.1(6).

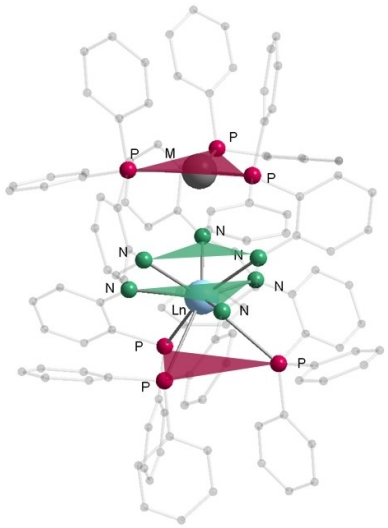

Figure 5. Presentation of the different coordination planes in the discussed compounds.

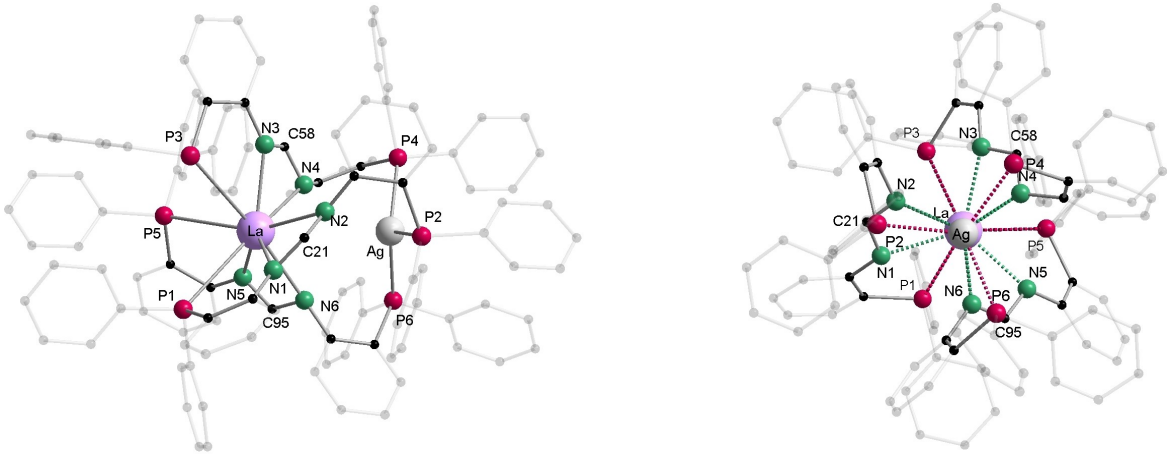

Figure 6. Molecular structure of **4** in the solid state from two different perspectives (for **5** see Figure S28). Protons, non-coordinating solvents and the counter anion are omitted for clarity. Selected bond lengths [Å] and angles [°] for **4** and **5**: **4**: La–P1 3.3675(9), La–P3 3.4326(10), La–P5 3.4088(9), La–N1 2.549(3), La–N2 2.698(3), La–N3 2.539(3), La–N4 2.663(3), La–N5 2.558(3), La–N6 2.664(3), Ag–P2 2.4864(8), Ag–P4 2.4934(9), Ag–P6 2.4829(9), N1–C21 1.338(4), N2–C21 1.320(4), N3–C58 1.337(4), N4–C58 1.326(4), N5–C95 1.332(4), N6–C95 1.312(4), N2–C21–N1 119.7(3), N4–C58–N3 120.1(3), N6–C95–N5 120.1(3), P2–Ag–P4 117.09(3), P6–Ag–P2 116.57(3), P6–Ag–P4 117.95(3). **5**: Nd–P2 3.3361(13), Nd–N1 2.639(3), Nd–N2 2.450(4), Ag–P1 2.4926(14), N1–C19 1.315(6), N2–C19 1.341(6), N2–C19–N1 118.2(4), P1–Ag–P1 116.60(2).

As the coordination pockets for the coinage metals formed by the P atoms in **1**, **4** and **5** are similar, our assumption that the coordination pocket in **1** is too small and too stiff for coordination seems to be reasonable.

The distance of the two metal centres in **4** and **5** is relatively short (La–Ag 4.05 Å and Nd–Ag 3.98 Å). Despite the fact that this is in the region of the sum of the corresponding van der Waals radii,[22] they are still too long to assume significant metal–metal interactions. Further insights will be gained by quantum chemical calculations (see below). Owing to the low solubility, $^{31}P\{^{1}H\}$ NMR spectra for **4** were recorded at elevated temperature (323 K; Figure S6 in the Supporting Information). One symmetric set of signals consisting of two outer broad resonances ($\delta = -12.4$ ppm and -21.0 ppm each integrating to ~1.5) and an inner set of resonances displaying a complex coupling pattern appearing as triplet of triplets (integrates to 3) is obtained. However, as the inner complex pattern ($\delta = -16.8$ ppm) conspicuously resembles the respective spectrum of [dpfam$_2$Ag$_2$] in terms of chemical shift, pattern and coupling constants,[15g] the presence of **4** in solution could not be unambiguously confirmed. Hence, also dynamic behaviour, involving [dpfam$_2$Ag$_2$] or a dissociation upon redissolving at elevated temperatures is possible. Therefore, the obtained spectra should be treated with care.

The hetero-bimetallic Ln–Au complexes [dpfam$_3$LnAu][OTf] (Ln = La (**6**), Nd (**7**)) were obtained analogously to **4** and **5** from the reaction of reactants **2** and **3** with bistetrahydrothiophene gold triflate [Au(tht)$_2$][OTf] (Scheme 3). The X-ray structural analysis for both compounds shows an approximately isostructural scaffold to the related silver compounds **5** and **6** (Figure 7).

The lanthanide cations are hence in the corresponding P_3N_6 coordination environments (muffin polyhedron) and the deviation of the P_3 and N_3 planes from a parallel orientation is at most 3.57° (Figure 7). Furthermore, the Ln–N bond lengths remain almost unchanged from **4** and **6** (∅(La–N) = 2.60 Å, ∅(Nd–N) = 2.53 Å). The gold cation is again located in a trigonal planar coordination environment which is observed rather scarcely for gold phosphines.[21,23] The determined P–Au–P angles are close to the ideal 120° (**5**: 120.43(4), 120.60(5), 115.74(6)°, **7**: 118.99(4), 119.66(4), 118.82(4)°) and a small Au–P_3 plane distance of ~0.2 Å is observed. The Au–P distances (**5**: Au–P1 2.3655(12), Au–P3 2.3871(14), Au–P5 2.3800(14) Å; **7**: Au–P2 2.3858(12), Au–P4 2.3860(12), Au–P6 2.3877(12) Å) are only slightly longer than those in the previous reported coinage metal complexes and agree well with literature values.[21]

Analogously to **4** and **5**, the Ln–M distances are again quite short but not small enough to suggest an interaction of the metal centres (La–Au 4.24 Å and Nd–Au 4.20 Å). Further discussion follows below in the context of quantum chemical calculations. As already observed for the silver compounds, the $^{31}P\{^{1}H\}$ NMR spectrum of **6** could not give certainty upon a retention of **6** in solution owing to its low solubility and possible dissociation/dynamic behaviour. The $^{31}P\{^{1}H\}$ spectrum at 323 K consists of two singlets at $\delta = 29.7$ and -9.7 ppm (Figure S10), which would fit the expectation of two different ^{31}P signals (Au- and La-coordinating phosphines, respectively).

Photoluminescence properties

To gain further insights into the properties of the hetero-bimetallic compounds their optical properties were investigated and compared to the respective lanthanide precursor. Photoluminescence (PL) and photoluminescence excitation (PLE) spectra were recorded at 77 K and room temperature for samples of **2**–**7** in the solid state. As organic ligands often serve as antenna for lanthanide based luminescence, a distinct

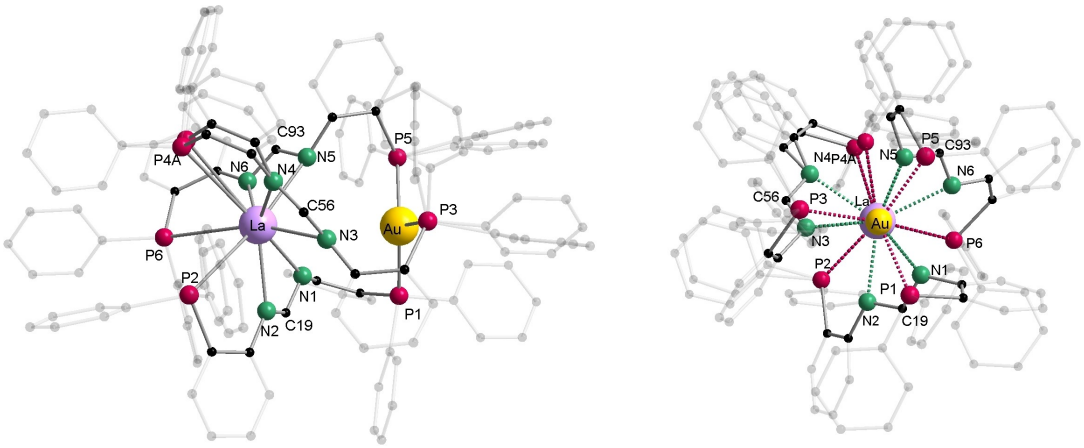

Figure 7. Molecular structure of **6** in the solid state from two different perspectives (for **7** see Figure S29). Protons, non-coordinating solvents and the counter anion are omitted for clarity. Selected bond lengths [Å] and angles [°] for **6** and **7**: **6**: La–P2 3.4234(14), La–P4 3.361(9), La–P6 3.481(2), La–N1 2.651(4), La–N2 2.525(4), La–N3 2.730(4), La–N4 2.541(4), La–N5 2.626(4), La–N6 2.554(4), N1–C19 1.319(6), N2–C19 1.331(6), N3–C56 1.309(6), N4–C56 1.333(6), N5–C93 1.328(6), N6–C93 1.315(6), Au–P1 2.3655(12), Au–P3 2.3871(14), Au–P5 2.3800(14), N2–C19–N1 119.4(4), N4–C56–N3 119.1(5), N5–C93–N6 119.9(4), P1–Au–P3 120.43(4), P1–Au–P5 120.60(5), P5–Au–P3 115.74(6). **7**: Nd–P1 3.3745(13), Nd–P3 3.3704(12), Nd–P5 3.3317(13), Nd–N1 2.459(4), Nd–N2 2.592(4), Nd–N3 2.481(4), Nd–N4 2.611(4), Nd–N5 2.466(4), Nd–N6 2.620(4), N1–C20 1.326(6), N2–C20 1.312(6), N3–C56 1.332(6), N4–C56 1.318(6), N5–C93 1.334(6), N6–C93 1.314(6), Au–P2 2.3858(12), Au–P4 2.3860(12), Au–P6 2.3877(12), N2–C20–N1 117.7(4), N4–C56–N3 118.9(4), N5–C93–N6 118.3(4), P2–Au–P4 118.99(4), P2–Au–P6 119.66(4), P4–Au–P6 118.82(4).

difference for **2** and **3** was expected.[24] Considering that for lanthanum there are no f-electrons available, for **2** only ligand based emission was expected. However, for **3**, if dpfam works successfully as antenna, distinct emissive f–f transitions in the IR region would be obtained.[25] Figure 8 shows the recorded spectra for Kdpfam and the samples **2** and **3**. Kdpfam expresses an intense and mostly temperature independent weakly structured emission band with a maximum at 437 nm. Excitation starts at ~440 nm. PL and PLE spectra for **2** and **3** are very similar to that of Kdpfam in terms of excitation energy and emission maximum. However, for **2** and **3** a strong decay in intensity is observed when warming up the sample and emission of Kdpfam covers a broader range tailing up to ~650 nm. Small Stokes shifts for all compounds indicate a fluorescence mechanism which is confirmed by short lifetimes <10 ns. For **3**, emission maxima in the IR area are observed at 898–915, 1070–1087 and 1344–1415 nm that can be assigned to the respective f–f transitions $^4I_{9/2}\leftarrow{}^4F_{3/2}$, $^4I_{11/2}\leftarrow{}^4F_{3/2}$ and $^4I_{13/2}\leftarrow{}^4F_{3/2}$ in accordance with literature.[25] For **4**, an additional long relaxation time was observed in the IR area, which could not be determined accurately but should be within the millisecond range.

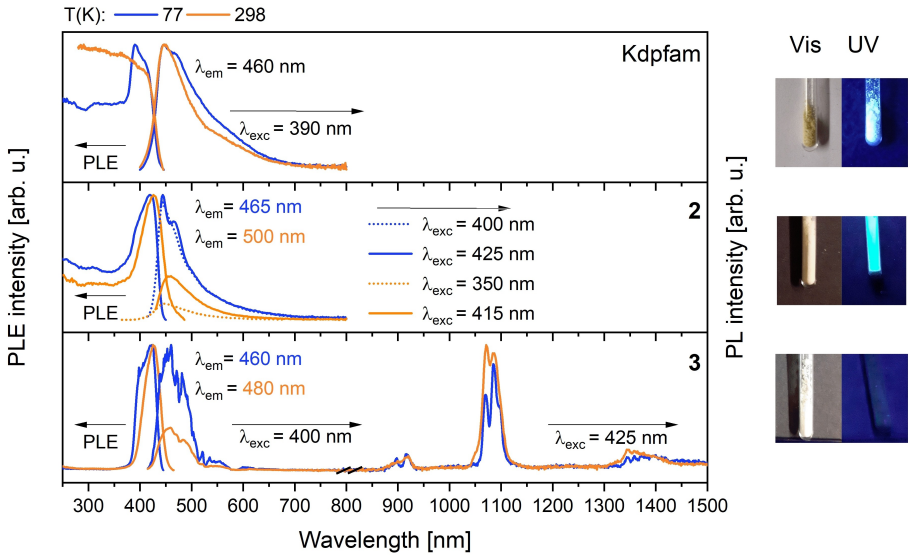

Figure 8. PL and PLE spectra of Kdpfam, **2** and **3** recorded at 77 K and room temperature at the given emission (PLE spectra λ_{em}) and excitation wavelengths (PL spectra λ_{exc}).

La^{3+} features no f-electrons and might therefore be compared to the alkali metals, resulting in very similar emission and excitation properties as Kdpfam. As Nd(III) is predominantly known for its IR emission, the expressed PL properties in the UV-vis area are assigned to the ligand system. Additional IR emission in **3**, not present for Kdpfam and **2**, based on Nd^{3+} centered transitions, shows successful energy transfer from dpfam working as antenna (Figure 8). Upon incorporation of the coinage metal, the difference in the expressed emission is striking (Figure 9).[15g] For **4**, vibronic structure and position of the emission band is nearly identical to [dpfam$_2$Ag$_2$] (Figure 2). It features a weaker emission band until approximately 480 nm and a more intense structured band until approximately 700 nm. First can be selectively excited by a shorter wavelength (λ_{exc} = 385 nm), while second is excited by longer wavelengths (λ_{exc} = 410 nm). Despite all similarities, the PLE band of **4** is more red shifted and features a different shape at room temperature than observed for [dpfam$_2$Ag$_2$].[15g] The PLE spectrum of **5** resembles at 77 K that of **4** but does not feature its distinct redshift at room temperature. Emission band of **5** appears as broad unstructured band and features a maximum that is slightly blue shifted compared to **4** but otherwise covering the same range-almost the whole visible area (400–700 nm).

In the NIR area (λ > 800 nm) none of the well-structured transitions from **3** remain for **5**. However, the maximum position remains unchanged at ~1070 nm. An increase in intensity from ~1400 nm indicates a possible further emission which is outside the detectors range. Surprisingly, also for **4** a broad signal was detected at 1000–1300 nm, roughly coping the same area as in **5**. As for Kdpfam and **2**, no NIR emission was observed this is tentatively assigned to the incorporation of the coinage metal. For **5**, the latter is probably overlaying the former distinct Nd^{3+} based transitions, resulting in one broad band. Lifetimes of **4** and **5** were determined to be < 5 ns and thus fluorescence based. An additional longer lifetime is visible but could not be determined due to insufficient intensity and overlaying of both signals.

Regarding the heterometallic gold compounds **6** and **7**, again a striking similarity with its homometallic relative [dpfam$_2$Au$_2$] (Figure 2) is visible. Excitation starts at ~430 nm and the emission maximum is at ~500 nm which is only slightly red shifted compared to [dpfam$_2$Au$_2$].[15g] Although PLE starts for **6** and **7** at approximately the same energy, the form and structure of the PLE bands differ from each other. While **7** features only one band (λ_{max} = 412 nm at 77 K), **6** expresses two excitation maxima (λ_{max1} = 380 nm, λ_{max2} = 415 nm at 77 K). As for **4**, when exciting with the shorter wavelength, a different emission spectrum is obtained which is blue shifted by ~30 nm compared to the PL spectrum obtained when exciting with 415 nm. Lifetimes at 77 K were determined to be $\tau_1 \approx 94$ µs und $\tau_2 \approx 609$ µs (λ_{exc} = 415 nm) for **6** and $\tau_1 \approx 78$ µs and $\tau_2 \approx 500$ µs for **7** which is slightly shorter than observed for [dpfam$_2$Au$_2$].[15g] Above 800 nm a similar observation is made as for the silver compounds. For both **6** and **7**, an IR emission is detected: while for **6** the band is unstructured with a maximum at ~1070 nm, **7** features the distinct Nd^{3+} emission peaks (896/926 nm and 1074/1104 nm) together with a broad band resembling the shape in **6**. Mentioned broad band might, analogously to the other hetero-bimetallic compounds, be assigned to a gold involved emission mechanism which is the only band observed for **4** and is overlayed with the Nd^{3+} based emission in **7**.

However, in order to obtain more precise information about the spectra and the influence of the two metal centres on these

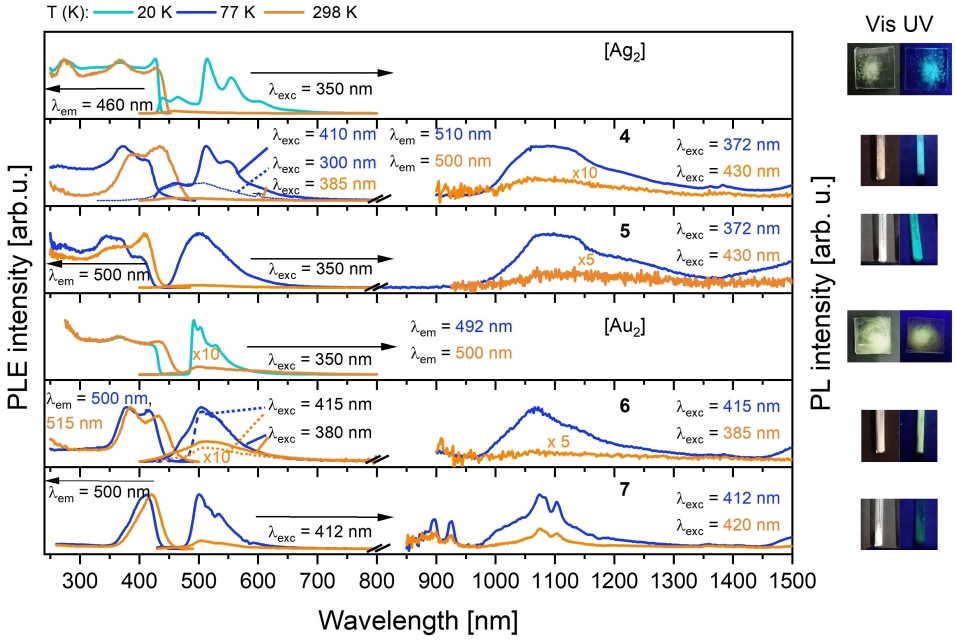

Figure 9. PL and PLE spectra of [dpfam$_2$Ag$_2$] (first row) and [dpfam$_2$Au$_2$] (forth row) from ref. [15] to compare with spectra of **4**–**7** recorded at 77 K and room temperature at the given emission (PLE spectra λ_{em}) and excitation wavelengths ((PL spectra λ_{ex}).

and on the excited states of the compounds, quantum chemical calculations were carried out.

Quantum chemical calculations

For a detailed analysis of the interaction between the coinage metal and the lanthanide atom, quantum chemical calculations were performed for molecules **4** and **6** with the program package TURBOMOLE.[26]

Geometry optimizations of **4** and **6** were performed applying different density functionals (BP and PBE0) and comparing results with and without dispersion corrections using Grimme's D3 approximation combined with Becke-Johnson damping (D3(BJ)).[27] Without dispersion interactions, the distance between the coinage metal and lanthanum is significantly too long (Tables S4 and S5). The Wiberg bond order (Table S6) is below 0.15.[28] The bond order as well as the too long bond distance without dispersion interactions indicate that there is no covalent metal-metal bond. For further analysis, model complexes were designed to distinguish between different types of interactions. The two models shown in Figure S27 were constructed to enable the use of the energy decomposition analysis[29] which gives individual contributions for electrostatic interaction, Pauli repulsion, orbital relaxation and dispersion interaction. This method is only applicable to analyse the interaction of two subsystems without a direct bond. Because of the bridging phenyl rings, **4** and **6** cannot directly be divided into such subsystems. Therefore, the bridging phenyl rings were removed and the dangling bonds saturated by hydrogen. In model **A**, the remaining phenyl rings were substituted by $-CH_3$ groups, while they were considered in model **B**. The subsystem with Au/Ag has a charge of $+1$ while the subsystem containing La is neutral. The energy decomposition analysis (EDA) was performed for three different structures, the experimental structure, the one optimized with BP–D3(BJ)/def2-TZVP* and without D3(BJ). The results are visualized in Figure 10, details are given in Tables S7 for **4** and S8 for **6**. Though the chemical bonds between the two parts of the molecules are now missing, changes connected to the metal-metal distance can still be observed.

Comparing different M/La distances within one of the models shows that the total interaction energy is only slightly decreasing with the distance, that is, the potential energy surface is flat. While significant changes are observed for the different contributions, the decrease in binding interactions (electrostatic, correlation and dispersion) and the exchange repulsion compensate each other to a large amount. The similar interaction energies of model **A** and **B** show that the non-bridging phenyl rings alone do not cause the short distance between the two parts of the molecule. Therefore, the dispersion energies of different groups of phenyl-rings (Figure S28, Tables S9 and S10) in the full molecules were analysed. As expected, the bridging phenyl-rings (red) and their interaction with those close by and marked in green and velvet in Figure S28 contribute with 1.6 eV in total to the dispersion interaction when using the structure optimized with D3(BJ). For

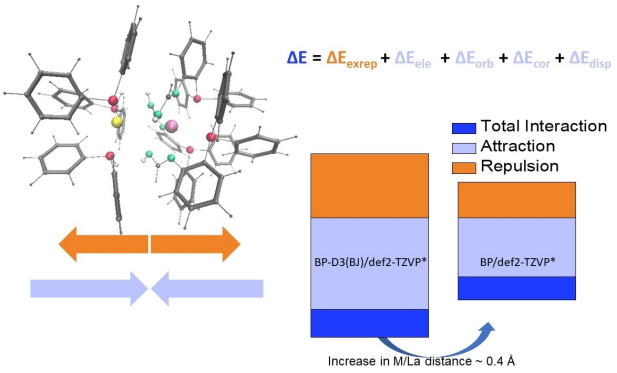

Figure 10. Results of the energy decomposition analysis[29] performed at the BP–D3(BJ)/def2-TZVP* level for model B with structures optimized with (BP–D3(BJ)/def2-TZVP*) and without (BP/def2-TZVP*) dispersion in the left and right columns of the bar graph, respectively. Blue: total interaction ΔE; orange: exchange-repulsion ΔE_{exrep}; velvet: attractive contributions: electrostatic interaction ΔE_{ele}, orbital relaxation ΔE_{orb}, correlation interaction ΔE_{cor} and dispersion ΔE_{disp}.

the long distance (based on the structure optimized without D3(BJ)) the contribution is reduced to 1.3 eV. (The values are similar for molecules **4** and **6**.) According to Table S11, the dispersion interaction between the metal centres is small (~ 0.05 eV).

Furthermore, we aimed for information about spectroscopic data. In the first step, singlet and triplet excited states were calculated at the ground state structure with the simplified TDDFT (sTDA) approach.[30] The results are summarized in Tables S15 and S16 for **6** and Tables S18 and S19 for **4**. In **4** and **6** the lowest excited states (ca. 3.5 eV) show a ligand-ligand transition (Figures S34 and S39).

In PL, the structure relaxes in the excited state before the emission takes place. To obtain information about these structural changes, the triplet states of **4** and **6** were optimized at DFT level and the singlet-triplet energy gap was calculated for the triplet structure. In **4**, the metal-metal distance only changed by 0.1 Å with a singlet-triplet gap of 2.57 eV. In the sTDA for the triplet structure, the first singlet and triplet excitation energies amount to 3.21 (386.7 nm) and 2.85 eV (435 nm), respectively.

For **6**, a singlet-triplet gap of 2.51 eV (494 nm) was obtained. The metal-metal distance is reduced significantly to 3.3 Å, (compared to 4.1 Å in the electronic ground state). The Wiberg bond order amounts to 0.21 in the triplet state indicating a stronger metal-metal interaction comparing to the ground state structure. The form of the spin density (shown in Table S14 and Figure S33) of the triplet state further supports the cooperativity of the metal centres in the excited state which can be classified as ligand to metal-metal charge transfer (LMMCT). This is in line with the sTDA calculations for the triplet structure (see information in Tables S12 and S13 and Figure S32). The lowest excitation was a HOMO-LUMO excitation which amounted to 2.65 eV (468 nm) for the singlet and 2.57 eV (482 nm) for the triplet excitation, respectively. In **6**, the origin of the lowest

excitation was a transfer from the amidinate ligand to the region between the metals shown in Figure 11.

In the case of the Nd complexes **5** and **7** the ligand field splitting of the 4f–4f transitions were calculated for a point charge field model by spin orbit configuration interactions at the ground state geometry.[31] The results are given in Figure S29. Here, the 4f–4f excitations are well known to be responsible for emissions in the IR range. In the calculations we performed so far, we did not find any transitions in that energy range for **4** and **6**.

In summary, the short metal–metal distance in the ground state does not originate from a metal-metal bond. As in a former study on a Pd–Lu complex,[12a] the origin for the short distance are interactions in the ligand system, in particular of the bridging ligands with the rest of the molecule.

Thus, there is no electron transfer from the soft Au^{I} ion to the hard lanthanides, which are Lewis acids. However, in the exited state the closed electron shell of the Au^{I} atom is opened and metal-to-metal interactions are observed.

Conclusions

A phosphine functionalized amidinate ligand system was used to synthesize hetero-bimetallic lanthanide-coinage metal compounds for the first time. We present a rare case in which hetero-bimetallic complexes of elements from the opposite edges of the d-block have been combined in a selective and stepwise manner. Starting from potassium-*N*,*N*′-bis[(2-diphenylphosphino)phenyl]formamidinate (Kdpfam), we have shown the synthesis of the compounds [$dpfam_3$LnM] (Ln = La, Nd), which have successfully been used as scaffolds for further selective incorporation of Ag^{+} and Au^{+}. By using this stepwise approach, lanthanides and coinage metals can be selectively introduced into the complexes. However, there are limitations due to the ligand geometry: i) for steric restrictions, only the larger lanthanides allow the generation of a suitable coordination pocket for the coinage metals; ii) for a selective coordination of the metals, there must be a significant difference in terms of soft and hard character of the metals used. Thus, Cu^{I} is not a suitable ion in this system.

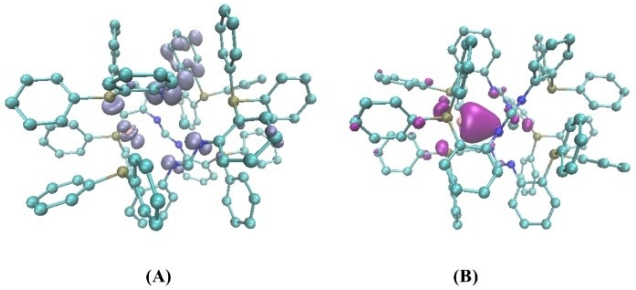

Figure 11. Transition of the lowest excited state obtained by sTDA at the triplet structure of complex **6**. In the excitation, electron density is shifted from the region of the ligand shown in A to the region between the metal centres (LMMCT).

The hetero-bimetallic compounds [$dpfam_3$LnM][OTf] (Ln = La, Nd and M = Ag, Au) feature a close proximity of the two metal centres of approximately 4 Å, and were investigated by photoluminescence spectroscopy and quantum chemical calculations. The PL spectroscopy results did not imply any interaction between the metal centres, neither did the calculations in the ground state. However, rare La-Au interactions for the first excited state of [$dpfam_3$LaAu][OTf] were found by the calculations, resulting in a shortened metal-metal bond length of 3.3 Å with a Wiberg bond order of 0.21.

Experimental Section

General experimental procedures for the synthesis of all compounds, details of the PL measurements and quantum chemical calculations as well as X-ray crystallography are described in the Supporting Information.

Deposition Numbers 2094624 (for **1**), 2094625 (for **2**), 2094626 (for **3**) 2094627 (for **4**), 2094628 (for **5**), and 2094629 (for **6**) and 2094630 (for **7**) contain the supplementary crystallographic data for this paper. These data are provided free of charge by the joint Cambridge Crystallographic Data Centre and Fachinformationszentrum Karlsruhe Access Structures service.

Acknowledgements

K.F. and P.W.R. gratefully acknowledge support by the Deutsche Forschungsgemeinschaft (DFG) through the Transregional Collaborative Research Centre 88 [Cooperative Effects in Homo- and Heterometallic Complexes (3MET)], Projects B1 and B3. N.R. and M.D. thank the Fonds der Chemischen Industrie for their generous support (nos. 102431 and 103581). Open Access funding enabled and organized by Projekt DEAL.

Conflict of Interest

The authors declare no conflict of interest.

Keywords: coinage metals · cooperativity · heterometallic · lanthanide · luminescence

[1] a) B. G. Cooper, J. W. Napoline, C. M. Thomas, *Catal. Rev.* **2012**, *54*, 1–40; b) P. Buchwalter, J. Rosé, P. Braunstein, *Chem. Rev.* **2015**, *115*, 28–126; c) A. Pinto, G. Spigolon, R. Gavara, C. Zonta, G. Licini, L. Rodríguez, *Dalton Trans.* **2020**, *49*, 14613–14625; d) Q. Xu, Z. Chen, H. Min, F. Song, Y.-X. Wang, W. Shi, P. Cheng, *Inorg. Chem.* **2020**, *59*, 6729–6735; e) P. B. Glover, P. R. Ashton, L. J. Childs, A. Rodger, M. Kercher, R. M. Williams, L. De Cola, Z. Pikramenou, *J. Am. Chem. Soc.* **2003**, *125*, 9918–9919; f) W. Zhou, J. W. Napoline, C. M. Thomas, *Eur. J. Inorg. Chem.* **2011**, *2011*, 2029–2033.

[2] a) R. G. Pearson, *J. Am. Chem. Soc.* **1963**, *85*, 3533–3539; b) R. G. Pearson, *Coord. Chem. Rev.* **1990**, *100*, 403–425.

[3] a) J.-C. G. Bünzli in *Handbook on the Physics and Chemistry of Rare Earths, Vol. 50* (Eds.: J.-C. G. Bünzli, V. K. Pecharsky), Elsevier, **2016**, pp. 141–176; b) J.-C. G. Bünzli, S. V. Eliseeva in *Lanthanide Luminescence: Photophysical, Analytical and Biological Aspects* (Eds.: P. Hänninen, H. Härmä), Springer, Berlin, **2011**, pp. 1–45.

[4] a) A. de Bettencourt-Dias, *Dalton Trans.* **2007**, 2229–2241; b) W. J. Mir, T. Sheikh, H. Arfin, Z. Xia, A. Nag, *NPG Asia Mater.* **2020**, *12*, 9; c) K. Binnemans, *Chem. Rev.* **2009**, *109*, 4283–4374.

[5] a) M. Suta, N. Harmgarth, M. Kühling, P. Liebing, F. T. Edelmann, C. Wickleder, *Chem. Asian J.* **2018**, *13*, 1038–1044; b) P. Dorenbos, *J. Lumin.* **2000**, *91*, 91–106; c) P. N. Hazin, C. Lakshminarayan, L. S. Brinen, J. L. Knee, J. W. Bruno, W. E. Streib, K. Folting, *Inorg. Chem.* **1988**, *27* (8), 1393–1400; d) H. G. Brittain, J. H. Meadows, W. J. Evans, *Organometallics* **2002**, *2* (11), 1661–1665.; e) J. H. S. K. Monteiro, A. Bettencourt-Dias, I. O. Mazali, F. A. Sigoli, *New J. Chem.* **2015**, *39*, 1883–1891; f) P. Dorenbos, A. H. Krumpel, E. van der Kolk, P. Boutinaud, M. Bettinelli, E. Cavalli, *Opt. Mater.* **2010**, *32*, 1681–1685; g) R. Lisiecki, *J. Lumin.* **2013**, *143*, 293–297; h) Y. Chen, Z. Xing, S. Cao, Y. Wang, *J. Rare Earth* **2016**, *34*, 240–244.

[6] C.-K. Li, X.-X. Lu, K. M.-C. Wong, C.-L. Chan, N. Zhu, V. W.-W. Yam, *Inorg. Chem.* **2004**, *43*, 7421–7430.

[7] a) V. W.-W. Yam, E. Chung-Chin Cheng in *Photochemistry and Photophysics of Coordination Compounds II, Vol. 281* (Eds.: V. Balzani, S. Campagna, A. Barbieri), Springer, Berlin, **2007**, pp. 269-309; b) H. Schmidbaur, A. Schier, *Angew. Chem. Int. Ed.* **2015**, *54*, 746–784; *Angew. Chem.* **2015**, *127*, 756–797.

[8] J. J. Jesudas, C. T. Pham, A. Hagenbach, U. Abram, H. H. Nguyen, *Inorg. Chem.* **2020**, *59*, 386–395.

[9] B. L. Ramirez, P. Sharma, R. J. Eisenhart, L. Gagliardi, C. C. Lu, *Chem. Sci.* **2019**, *10*, 3375–3384.

[10] K. Shi, I. Douair, G. Feng, P. Wang, Y. Zhao, L. Maron, C. Zhu, *J. Am. Chem. Soc.* **2021**, *143*, 5998–6005.

[11] R. Kempe, H. Noss, H. Fuhrmann, *Chem. Eur. J.* **2001**, *7*, 1630–1636.

[12] a) F. Völcker, F. M. Mück, K. D. Vogiatzis, K. Fink, P. W. Roesky, *Chem. Commun.* **2015**, *51*, 11761–11764; b) F. Völcker, P. W. Roesky, *Dalton Trans.* **2016**, *45*, 9429–9435.

[13] B. Oelkers, M. V. Butovskii, R. Kempe, *Chem. Eur. J.* **2012**, *18*, 13566–13579.

[14] a) M. Gregson, E. Lu, D. P. Mills, F. Tuna, E. J. L. McInnes, C. Hennig, A. C. Scheinost, J. McMaster, W. Lewis, A. J. Blake, A. Kerridge, S. T. Liddle, *Nat. Commun.* **2017**, *8*, 14137; b) N. Iki, M. Ohta, T. Horiuchi, H. Hoshino, *Chem. Asian J.* **2008**, *3*, 849–853; c) M. Maity, M. C. Majee, S. Kundu, S. K. Samanta, E. C. Sañudo, S. Ghosh, M. Chaudhury, *Inorg. Chem.* **2015**, *54*, 9715–9726; d) R. J. Roberts, X. Li, T. F. Lacey, Z. Pan, H. H. Patterson, D. B. Leznoff, *Dalton Trans.* **2012**, *41*, 6992–6997; e) N. Iki, S. Hiro-oka, T. Tanaka, C. Kabuto, H. Hoshino, *Inorg. Chem.* **2012**, *51*, 1648–1656.

[15] a) N. Tsukada, O. Tamura, Y. Inoue, *Organometallics* **2002**, *21*, 2521–2528; b) L. Wesemann, H. Schubert, H. Mayer, S. Wernitz, Deutsches Patent- und Markenamt, DE 10 2011 079 857 A1, **2011**; c) K.-S. Son, D. M. Pearson, S.-J. Jeon, R. M. Waymouth, *Eur. J. Inorg. Chem.* **2011**, 4256–4261; d) S. Tanaka, A. Yagyu, M. Kikugawa, M. Ohashi, T. Yamagata, K. Mashima, *Chemistry* **2011**, *17*, 3693–3709; e) Y. Yamaguchi, K. Yamanishi, M. Kondo, N. Tsukada, *Organometallics* **2013**, *32*, 4837–4842; f) M. Dahlen, E. H. Hollesen, M. Kehry, M. T. Gamer, S. Lebedkin, D. Schooss, M. M. Kappes, W. Klopper, P. W. Roesky, *Angewandte Chem. Int. Ed.* 10.1002/anie.202110043; g) M. Dahlen, M. Kehry, S. Lebedkin, M. M. Kappes, W. Klopper, P. W. Roesky, *Dalton Trans.* **2021**, 10.1039/D1DT02226A.

[16] a) G. R. Choppin, D. R. Peterman, *Coord. Chem. Rev.* **1998**, *174*, 283–299; b) C. R. Kesavulu, A. C. Almeida Silva, M. R. Dousti, N. O. Dantas, A. S. S. de Camargo, T. Catunda, *J. Lumin.* **2015**, *165*, 77–84; c) J. H. S. K. Monteiro, A. de Bettencourt-Dias, I. O. Mazali, F. A. Sigoli, *New J. Chem.* **2015**, *39*, 1883–1891.

[17] SHAPE 2.1 for Windows (32 bit), M. Llunell, P. Alemany, S. Alvarez, http://www.ee.ub.edu/index.php?option=com jdownloads&view=-viewcategories&Itemid=529, accessed 30.6.2021.

[18] a) X. Pang, H. Sun, Y. Zhang, Q. Shen, H. Zhang, *Eur. J. Inorg. Chem.* **2005**, 1487–1491; b) P. Dröse, S. Blaurock, C. G. Hrib, L. Hilfert, F. T. Edelmann, *Z. Anorg. Allg. Chem.* **2011**, *637*, 186–189; c) J.-F. Liu, F.-X. Pan, S. Yao, X. Min, D. Cui, Z.-M. Sun, *Organometallics* **2014**, *33*, 1374–1381.

[19] T. D. Tilley, R. A. Andersen, A. Zalkin, *J. Am. Chem. Soc.* **1982**, *104*, 3725–3727.

[20] a) C. Qian, X. Zhang, J. Li, F. Xu, Y. Zhang, Q. Shen, *Organometallics* **2009**, *28*, 3856–3862; b) T. S. Brunner, P. Benndorf, M. T. Gamer, N. Knöfel, K. Gugau, P. W. Roesky, *Organometallics* **2016**, *35*, 3474–3487; c) G. G. Skvortsov, A. O. Tolpygin, D. M. Lyubov, N. M. Khamaletdinova, A. V. Cherkasov, K. A. Lyssenko, A. A. Trifonov, *Russ. Chem. Bull.* **2017**, *65*, 2832–2840.

[21] a) A. Straube, P. Coburger, M. R. Ringenberg, E. Hey-Hawkins, *Chem. Eur. J.* **2020**, *26*, 5758–5764; b) M. N. I. Khan, R. J. Staples, C. King, J. P. Fackler, R. E. P. Winpenny, *Inorg. Chem.* **1993**, *32*, 5800–5807.

[22] a) A. Bondi, *J. Phys. Chem.* **1964**, *68*, 441–451; b) S.-Z. Hu, Z.-H. Zhou, B. E. Robertson, *Z. Kristallogr.* **2009**, *224*, 375–383.

[23] M. Concepción Gimeno, A. Laguna, C. Sarroca, P. G. Jones, *Inorg. Chem.* **1993**, *32*, 5926–5932.

[24] J. P. Leonard, C. B. Nolan, F. Stomeo, T. Gunnlaugsson, in *Photochemistry and Photophysics of Coordination Compounds II* (Eds.: V. Balzani, S. Campagna), Springer, Berlin, **2007**, pp. 1–43.

[25] R. N. A. Prasad, R. Praveena, N. Vijaya, P. Babu, N. Krishna Mohan, *Mater. Res. Express* **2019**, *6*, 096204.

[26] TURBOMOLE V7.4.1 2019, TURBOMOLE GmbH, 1989–2007, University of Karlsruhe and Forschungszentrum Karlsruhe GmbH, http://www.turbomole.com, accessed 30.6.2021.

[27] a) S. Grimme, J. Antony, S. Ehrlich, H. Krieg, *J. Chem. Phys.* **2010**, *132*, 154104; b) S. Grimme, S. Ehrlich, L. Goerigk, *J. Comput. Chem.* **2011**, *32*, 1456–1465.

[28] K. B. Wiberg, *Tetrahedron* **1968**, *24*, 1083–1096.

[29] P. Su, H. Li, *J. Chem. Phys.* **2009**, *131*, 014102.

[30] S. Grimme, *J. Chem. Phys.* **2013**, *138*, 244104.

[31] a) T. Bodenstein, *Entwicklung und Anwendung von Multireferenzverfahren zur Beschreibung magnetischer Eigenschaften von Metallkomplexen*, Karlsruhe Institute of Technology **2015**; b) T. Bodenstein, K. Fink, A. Heimermann, C. van Wüllen, **2021**, accepted by ChemPhysChem with DOI DOI: 10.1002/cphc.202100648.

Manuscript received: July 6, 2021
Accepted manuscript online: July 30, 2021
Version of record online: September 12, 2021

